

# Sub-Salt AVO and Seismic Inversion analysis: An example from deep water, Gulf of Mexico.

Simon Oropeza\* , Ianthe Sarrazin and Ricardo Campos, Petrobras America Inc.

Copyright 2009, SBGf - Sociedade Brasileira de Geofísica

This paper was prepared for presentation during the 11<sup>th</sup> International Congress of the Brazilian Geophysical Society held in Salvador, Brazil, August 24-28, 2009.

Contents of this paper were reviewed by the Technical Committee of the 11<sup>th</sup> International Congress of the Brazilian Geophysical Society and do not necessarily represent any position of the SBGf, its officers or members. Electronic reproduction or storage of any part of this paper for commercial purposes without the written consent of the Brazilian Geophysical Society is prohibited.

## Abstract

Deep water exploration efforts in the Gulf of Mexico (GOM) are challenged by illumination limitations of sub-salt prospects especially if wide azimuth seismic data is not available. In spite of the modern technological advances in imaging of narrow azimuth 3D seismic data, which is usually available at relatively low cost in the GOM, questions are raised on whether it contains enough angle of incidence information as to be used in amplitude and rock physics analysis. Higher angle of incidence becomes an issue due to the lack of amplitude information in mid-far and far traces needed for fluid interpretation. This paper analysis the scopes of the AVO and pre-stack seismic inversion studies in sub-salt exploration using narrow azimuth 3D seismic data.

## Introduction

The example shown here comes from ultra deep water in the Gulf of Mexico where two exploratory wells have been recently drilled. The target reservoir in both wells consists of Sub-salt Lower Pliocene sand bodies in an environment where faulting and folding associated with salt tectonics constitute the main trapping mechanism.

The salt cap in one of the wells (well A) is 5155 ft, and the water column is 7550 ft. The reservoir zone includes an upper low impedance gas-oil sand separated from a lower massive sand bearing about 15 m of oil (see figure 1).

A decrease in the acoustic impedance log is observed toward the top of the upper reservoir where the presence of gas has been confirmed. The increase in acoustic impedance toward the bottom of the sand is associated with oil.

The Poisson's ratio log decreases from the top of the gas sand to a minimum that coincides with the maximum value of resistivity and then increases to values of the background trend until it reaches the top of the oil sand when decreases slightly compared to the gas sand.

The second well (well B) is located at a distance of 4.8 km from well A in a structurally complex zone, below 9450 ft of salt, characterized by poor illumination. The reservoir is an oil-bearing low impedance massive sand showing oil at different levels. Poisson's ratio decreases slightly at each level especially toward the top of the sand as shown on figure 2.

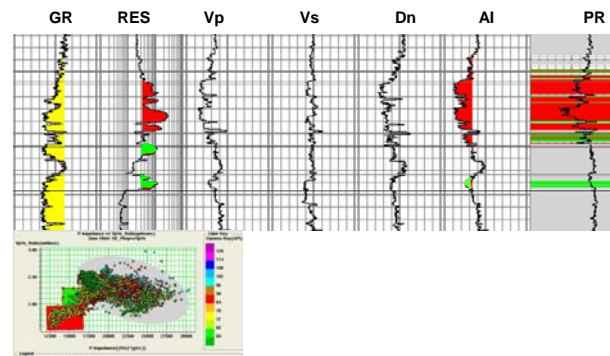


Figure 1.- Well A acoustic impedance vs Vp/Vs cross-plot highlights the reservoir zones. Notice the decrease on the Poisson's ratio at reservoir levels. GR= Gamma Ray, RES= Deep Resistivity, Vp and Vs = Compressional and Shear Velocity, Dn = Density, AI= Acoustic Impedance, PR= Poisson's ratio.

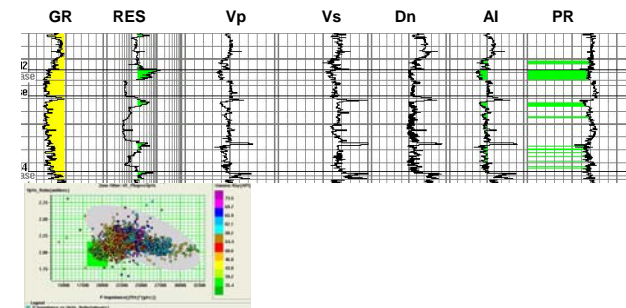


Figure 2. Well B acoustic impedance vs. Vp/Vs cross-plot highlights the reservoir zones. Notice the decrease on the Poisson's ratio at reservoir levels. GR= Gamma Ray, RES= Deep Resistivity, Vp and Vs = Compressional and Shear Velocity, Dn = Density, AI= Acoustic Impedance, PR= Poisson's ratio

## The Workflow

A conventional pre-stack amplitude analysis approach includes well data preparation, pre-stack seismic conditioning, well modeling and interpretation. The workflow is integrated through a geological-geophysical model as summarized on figure 3.

The compression, and shear velocity logs as well as the density logs were available for both wells. Minor editing was required to remove undesirable spikes.

Pre-stack depth migrated (PSDM) gathers were available for this study. The data required additional mute to remove noisy energy from the far traces. Super gather was a process used in an attempt to enhance the data

followed by trim static to flatten the seismic events at target depth. An offset scaling function based on the RMS amplitude of the background trend estimated from synthetic gathers was applied to minimize amplitude variability from the near to the mid traces. Offset gathers were then converted to angle gathers by using seismic RMS velocities.

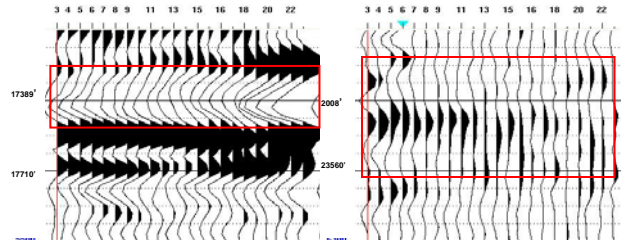


Figure 4. Angle Gather at well A and B. The seismic amplitude at well B is dramatically weakened by a combination of factors that include structural position, depth and salt thickness. The red rectangles highlight the reservoir zone.

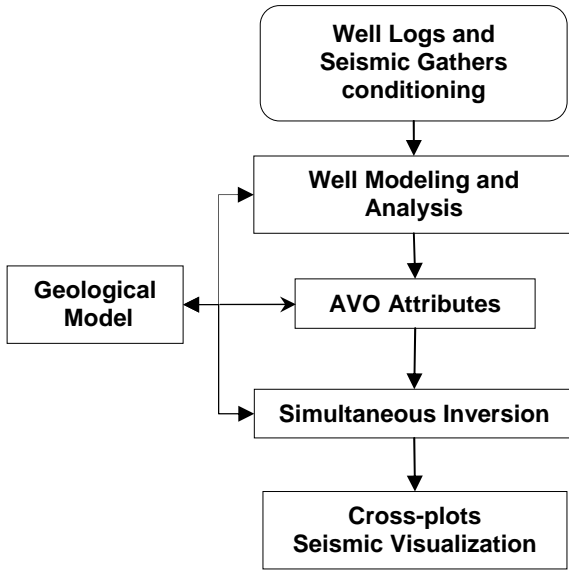


Figure 3. General workflow.

**Angle of Incidence**

Muerdter et al., 2001, showed that the maximum sub-salt angle of incidence decreases with increased thickness of salt. For dipping salt, the illumination decreases as the dip increases. Ray tracing modeling by the same author shows that the amplitude decreases with the offset being dramatically decreased for far traces. Moreover, the AVO response is controlled by the dip of salt, and the shooting direction with down dip having smaller amplitude. Comparison of gathers at well A and well B (figure 4), illustrates how the amplitude is affected by the structural position and thickness of the salt in the area surrounding well B. The gather at well A, however shows usable amplitude information up to about 23°.

Let's now consider the 2-terms Shuey's approximation which is a simplified version of the Zoeppritz's equation and expresses the reflectivity as a function of the incident angle ( $\theta$ ):

$$R(\theta) = A + B * \sin^2(\theta) \tag{1}$$

Where R is the Reflectivity, A is the intercept and B is the gradient.

The solution of equation 1 is obtained by lineal fitting of seismic amplitude as a function of the square sine angle of incidence. The ideal case would be a data set with no amplitude dispersion from the near to the far traces in which two points would be needed to solve for the intercept and the gradient. However, due to acquisition foot print, noise, seismic dispersion, etc., the reality is far from this ideal scenario and the solution will rely on the best fit that can be achieved by least square solution of equation 1.

Near traces will contribute to the intercept, thus in a data set where neither mid nor far traces exist the solution of the gradient term will not be usable. If the data shows low amplitude variability, the near to mid traces will be sufficient to obtain a reliable solution of the intercept and the gradient. A practical used method to reduce amplitude variability is offset scaling. Figure 5 shows the effect of applying an offset-dependant scaling factor to the gather located at well A. Observe the low amplitude and high dispersion at far traces. The far amplitude is not usable for AVO analysis or pre-stack inversion. However, near to mid amplitude information can be used in the area surrounding well A.

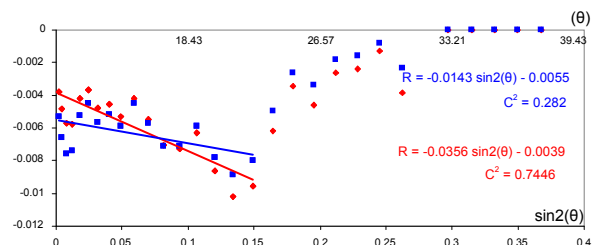


Figure 5. Amplitude vs.  $\sin^2(\theta)$  for the gather at well A. Blue is the amplitude without offset scaling and red is the amplitude after applying an offset-dependent scalar

**AVO Modeling**

A cross plot of acoustic impedance vs. Vp/Vs ratio shows that the gas sand is clearly distinguishable from the background trend while Oil sand lies closer to the background trend. The question is: Could we resolve gas sand and oil sand seismically using AVO and pre-stack seismic attributes? The answer is investigated through well modeling.

Well modeling was performed on both wells simulating the same reservoir conditions and considering that the maximum incidence usable angle from the actual seismic gathers lies between 23 to 25 around well A and 15 to 18 degrees around well B.

Synthetic AVO modeling based on Fluid Replacement indicates that it is possible to use AVO attributes to identify the top of the upper gas sand in well A. According to the classification model proposed by Rutherford et al., 1989, the top of this sand is interpreted as a class III sand type with low gradient. The gas synthetic gather and the actual gather at well location show similar behavior; that is, negative amplitude increasing with offset that is differentiable from the amplitude behavior of the brine and oil cases.

In spite of the low incidence angle range, it is possible to identify the top of the gas sand through AVO attributes analysis.

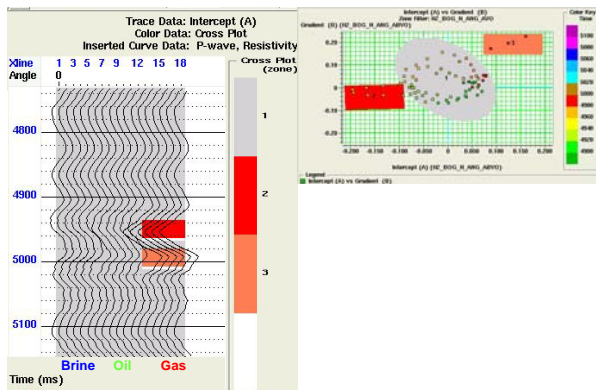


Figure 6. Well A color zones from the synthetic A vs. B cross-plot. Red is the top of the gas sand in well A. Oil can not be differentiated from the background trend.

**AVO Attributes**

Having conditioned angle gathers, the intercept and gradient attributes were obtained by the solution of the two terms-Aki-Richard's equation. The third term was neglected due to the low range of usable angle of incidence.

As mentioned before, low variability amplitude data from near to mid and far traces will provide a good linear fit. The amplitude variation from the near to the mid traces in the area around well A is considered moderate thus the gradient attribute will be usable under the premises that low amplitude variability will produce a reliable solution of the gradient.

There is no doubt about the fact that having a wide range of incident angles from near to far and ultra far traces will

increase the confidence on the AVO attributes but considering the operational and practical conditions of the available pre-stack data, near to mid traces can be used to obtained reliable AVO attributes.

An A vs. B colored coded seismic line through well A (figure 7) shows that mid traces can be used to generate AVO attributes. Due to the lack of mid and far traces around well B, the AVO attributes are not useful. This is extended to pre-stack inversion as only near traces are present. The difference is that the usable angle of incidence in well B reaches a maximum of 6°-7°. Low amplitude and noise also characterize the data around well B.

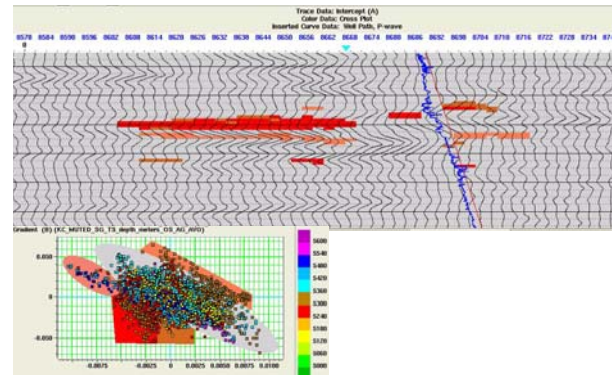


Figure 7.- A vs. B color-coded seismic line across well A. Traces correspond to the intercept and colors correspond to the A vs. B cross-plot zones.

**Pre-Stack Seismic Inversion**

Knowing the limitations on the data due to the lack of far traces to solve for the density term, seismic inversion was performed in an attempt to use the available pre-stack information efficiently. Pre-stack data as opposed to partial stack data has the advantage of bearing more amplitude information as more data is used in the inversion process.

The PSDM gathers previously used to compute the AVO attributes were converted from depth to time by using the RMS velocity volume available for this data set. Well-seismic correlation was performed and two wavelets, representing the near and mid traces, were extracted from the seismic and well data.

Due to the noisy nature of the seismic data and the low angle of incidence range around well B, the Acoustic impedance is the only reliable attribute in the surrounding area. For well A the Vp/Vs solution seems to be stable and reliable.

A model-based inversion algorithm that uses a modified version of the Aki-Richard's equation was used to obtain the acoustic impedance, shear impedance and Vp/Vs volumes.

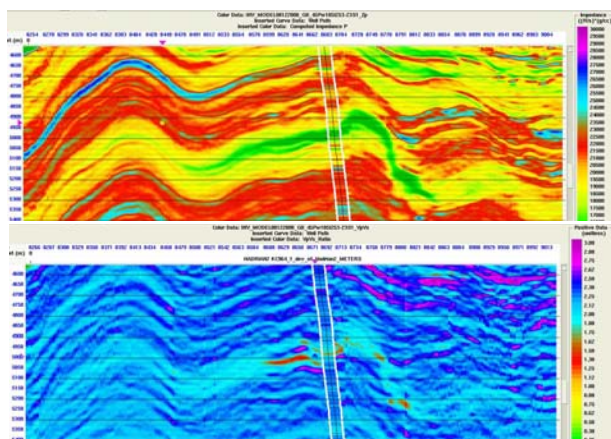


Figure 8. Pre\_stack inverted acoustic impedance (top) and Vp/Vs volume (bottom) across Well A. The acoustic impedance and Vp/Vs logs are superimposed for reference. The reservoir zone shows low impedance and low Vp/Vs.

Acoustic impedance lines (top) across well A and well B are shown on figures 8 and 9. The line across well A shows a low impedance interval consistent with the well data. The interval includes the top gas sand and the lower oil sand. Vp/Vs inverted lines across well A and B are also shown on figures 8 and 9. The low Vp/Vs values are consistent with the pay zone at well A.

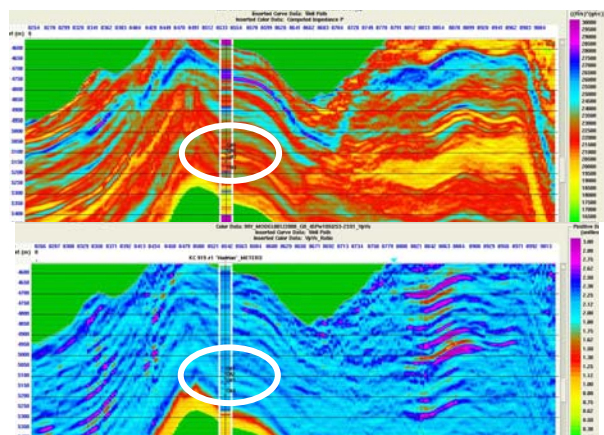


Figure 9.- Pre-stack inverted acoustic impedance (top) and Vp/Vs volume (bottom) across Well B. The acoustic impedance and Vp/Vs logs are superimposed for reference. No response is observed at the reservoir zone (white ellipse).

## Conclusions

Deep water exploration faces the limitations of seismic imaging that becomes critical for sub-salt prospect identification and evaluation. The lack of wide azimuth data brings uncertainties and unreliability to the AVO analysis and pre-stack seismic inversion in a particular area. However, if usable amplitude data with low to moderate amplitude variability is available from the near to mid traces it is possible to obtain reliable AVO and inversion attributes as it has been presented in this paper.

## Acknowledgments

The author would like to thank Petrobras America Inc., for permission to show the data.

## References

- Castagna, J., Batzle, M., and Eastwood, R., 1985, Relationships between compressional-wave and shear-wave velocity in clastic silicate rocks: *Geophysics*, Vol. 50, No. 4, 571-581
- Muerdter, D., et al, 2001, Understanding Subsalt illumination through ray-trace modeling, Part 2: Dipping salt bodies, salt peaks, and nonreciprocity of subsalt amplitude response: *The Leading Edge*, 688-697.
- Rutherford, S., and Williams, R., 1989, Amplitude-versus-offset variations in gas sand: *Geophysics*, Vol., 54, No. 6, 680-688.
- Shuey, R., 1985, A simplification of the Zoeppritz equations: *Geophysics*, Vol., 50, No. 4, 609-614.
- Smith, T., Sondergeld, C., and Rai C., Gassman fluid substitutions: A tutorial: *Geophysics*, Vol., 68, No. 2, 430-440.
- Van Koughnet, R., and Ford, D., 2001, Deep wells in deep water: Gulf of Mexico rock property observations / AVO implications: *SEG Expanded Abstract*, 20-247.